Iranian Journal of Materials Science and Engineering, Vol. 20, Number 1, March 2023

RESEARCH PAPER

Physical Properties of Reactively Sputter-Deposited C-N Thin Films

N. Aklouche[1,*], A. Mosbah[2]

* *nadjet.aklouche@setif-univ.dz*

[1] Laboratoire d'Elaboration de nouveaux matériaux et leurs caractérisations, Université Ferhat Abbas Sétif 1, Sétif, 19000, Algeria

[2] Laboratoire d'Etude des surfaces et interfaces des matériaux solides, Université Ferhat Abbas Sétif 1, Sétif, 19000, Algeria

Received: May 2022 **Revised: November 2022** **Accepted: December 2022**

DOI: 10.22068/ijmse.2803

Abstract: *The aim of this work was to prepare and study amorphous carbon nitride (CNx) films. Films were deposited by reactive magnetron radiofrequency (RF) sputtering from graphite target in argon and nitrogen mixture discharge at room temperature. The ratio of the gas flow rate was varied from 0.1 to 1. Deposited films were found to be amorphous. Highest Nitrogen concentration achieved was 42 atomic percent which is very rare and therefore, the highest nitrogen to carbon atomic ratio was 0.76. The incorporation of nitrogen promoted the clustering of diamond-like sites at the expense of graphitic sites leading to a decrease in disorder. The film surface became rougher with the increase nitrogen concentration. Films were optically transparent in the 200-900 nm wavelength range with a wide gap varying between 3.59 and 3.63 eV. There was an increase in resistivity from 15 to 87.4 × 10^{-3} Ω. cm for a-CN_x thin films for 0.1< R_F< 0.8 and a less decrease for R_F >0.8. Pore size increased in the films, but had little influence on band gaps. On the other hand, increased pore size reduced electrical interaction between particles by increasing resistivity.*

Keywords: *carbon nitride, reactive magnetron RF sputtering, structural properties, optical properties.*

1. INTRODUCTION

Quite recently, considerable attention has been paid to carbon nitride thin films. The observed properties have provided evidence for potential use in optoelectronic devices such as electro-luminescence devices and photovoltaic solar cells [1]. In this regard, the optical characteristics of these films have attracted a lot of interest [2].

What we know about carbon- rich carbon nitride films is largely based upon empirical study carried out by Liu and Cohen in the 1990s [3]. In fact, they predicted the development of a β-C_3N_4 structure with properties comparable to those of diamond. Indeed, this structure is not yet well evidenced, despite several publications on this subject.

Carbon nitride films have been studied as hard protective coating materials for rigid magnetic storage disks and as long-life charge stripper foils for tandem accelerators [4]. Carbon nitride films, in particular, may be utilized as antireflection coating for c-Si solar cells given to their indirect band gap, high thermal stability, great mechanical strength, high transmission, and low reflectivity, as well as their ease of manufacturing using reactive magnetron sputtering [5].

This study aims to enrich this growing area of research by showing an important contribution.

In this paper, a technique that improves the formation of amorphous carbon nitride thin films, deposited by reactive radio-frequency magnetron sputtering under different nitrogen flow rate, has been presented. However very few publication, can be found in the literature, that discuss this method especially on carbon nitride thin films. Magnetron sputtering has become the process of choice for the deposition of a wide range of industrially important coatings and it is preferred for industrial applications because of its simplicity and its use for deposition of many materials [6-8].

The magnetron source developed in the 1970s represents a significant advance in the efficiency of sputter tooling. The magnetron uses strong magnetic fields which usually come from permanent magnets, to keep secondary electrons confined spatially close to the target surface. By confining the secondary electrons near the surface of the target, its residence time in the plasma is much longer, leading to higher ionization of the plasma particles of sputter steam, thicker plasma, higher plasma currents and deposition speeds.

In a magnetron sputter source, the high electrical field resulting from the fall potential of the cathode Accelerates secondary electrons in a

normal direction to the target surface.
The configuration of the magnetic field is specifically developed so that the parallel field lines to the target surface, resulting in an ExB drift forces applied on the secondary electrons. The electrons are therefore confined to spiral motion drift orbits parallel to the target surface, resulting in additional collisional ionization of the sputter-gas atoms and higher overall plasma currents [9].
Reactive sputtering can be used to deposit films at room temperature; essential for optical and electronic structures. This method consists to deposit materials by adding gas to the sputtering chamber. The carbon nitride films can be produced by reactive sputtering using argon-nitrogen plasma. Despite all existing synthesis techniques, films with high nitrogen content are not easily achievable. Reports indicate that nitrogen rates exceeding 40 at. % are uncommon [10, 11]. In addition, most of the efforts result mainly in amorphous microstructures or even sometimes nano-sized crystalline clusters embedded in the amorphous matrix [12, 13].

2. EXPERIMENTAL PROCEDURES

2.1. Film Deposition

Reactive magnetron radiofrequency sputtering method was used to deposit carbon nitride thin films using Alcatel SCM 450 sputtering apparatus at 13.56 MHz frequency in different argon-nitrogen gas atmospheres at room temperature. In our work, the deposition process takes place in a vacuum chamber where the target and substrate are placed. A commercial graphite target of 99.999% purity, 100 mm diameter and 6 mm thickness was used. Before the deposition, the sputtering chamber was evacuated down to 10^{-6} mbar, the plasma power has been set at 100 W and the deposition pressure was fixed at 10^{-2} mbar. The deposits were made over a period of 15 min, at room temperature and the ratio of the gas flow rate $R_F = F_{N_2}/(F_{Ar} + F_{N_2})$ varies between 0.1 and 1, where F_{N_2} and F_{Ar} are the flows of nitrogen and argon, respectively. The target's distance from the substrate was set at 122 mm.
Thin films were deposited on various substrates: silicon for thickness, optical and Atomic Force Microscopy (AFM) characterizations, silicon wafer for Fourier-transform infrared spectroscopy (FTIR) and X-ray diffraction (XRD) measurements, quartz for Electron Spin Resonance (ESR) and finally vitreous carbon for Rutherford backscattering spectrometry (RBS).

2.2. Characterization of Films

The structure of prepared samples was investigated using an X'Pert PRO X-ray diffractometer with a Cu K_α anticathode and X'Celerator linear detector. The detector's scanning angle was varied between 10° and 60° with a step size of 0.0017°. The thicknesses of the deposited layers were measured with a DEKTAK 150 profiler. In this apparatus, the surface to be studied is scanned by a diamond tip; the probe has a lateral deflection of 4 nm and a vertical resolution of 5 nm.
Rutherford backscattering (RBS) with 2 MeV alpha particles and 15 nA current intensity was used to examine the layer composition; a charge of 10 µC was collected at 165° detection angle. There is no overlapping in the RBS signal of the graphite substrate, which appears at a lower energy than the constituents of the film. We should mention that RBS is a restricted approach, with a depth resolution of about 5 to 10 nm. As a result, this method is unsuitable for studying materials in very thin layers, and it involves some errors.
The experimental spectra are processed using the SIMNRA simulation program [14]. For a better fit of the theoretical one to the experimental spectrum, the thin film can be subdivided into sub-layers parallel to the surface, of adjusted thickness and composition.
Film roughness was determined by Atomic Force Microscopy using Asylum MFP-3D AFM apparatus.
The bonding structure was evaluated by a thermo Nicolet 5700 Fourier Transform Infra-red (FTIR) spectrometer in the range 400-4000 cm^{-1} with 4 cm^{-1} resolution. After subtracting a linear background, the FTIR spectra were fitted with Gaussian functions to determine the contributions of important band.
Electron Spin Resonance (ESR) measurements of films deposited on quartz substrates were carried out using a Bruker EMX ESR spectrometer, with a microwave frequency of 9.653 GHz (X-band) and a microwave power of 6.35 mW with a modulation amplitude of g= (2.0036 ± 0.0002), at a frequency of 100 kHz. The data were recorded and then simulated using Bruker WIN-EPR and SIMFONIA software, respectively.

Optical gap and Urbach energy were extracted from transmittance spectra obtained from a UV–Vis Perkin-Elmer spectrophotometer in the wavelength range extending from the region of the near-infrared (1100 nm) to the ultraviolet (200 nm).

3. RESULTS AND DISCUSSION

In this study, the abbreviation a-CN_x will be used to refer to amorphous carbon nitride films; with x is N/C atomic ratio.

3.1. Structural Properties

Initially, the X-Ray Diffraction investigation reveals that the spectrum, as shown in Figure 1, avoids sharp peaks, suggesting that the films are amorphous in nature. For practical applications, amorphous carbon films are very significant, for example, in the application of magnetic thin film recording disk overcoat [15] and for solar cell devices [16]. The great majority of the deposits have been found to be amorphous [17].

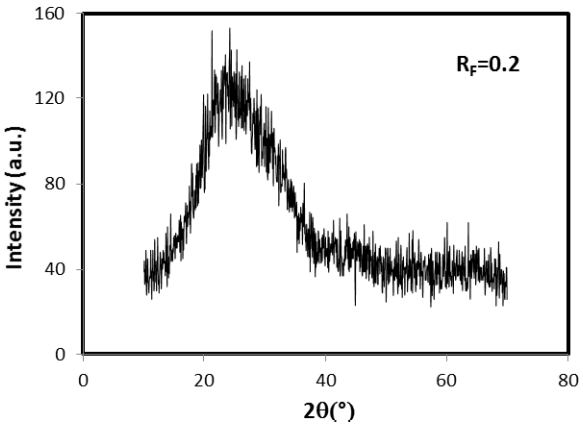

Fig. 1. XRD Spectrum of a-CN_x for R_F= 0.2

The thickness measurements allowed us to calculate the deposition rate of the layers. The deposition rate is a very good parameter to follow the evolution of the deposition process and to predict the nature of the deposited material.

As shown in Figure 2, two different areas can be defined. Initially, the deposition rate of the thin layers of a-CN_x increases with the increase of gas flow rate R_F. Indeed, values ranging from about 1.8 to 11.7 nm min^{-1} were obtained when the gas flow rate R_F was varied from 0.1 to 1. This can be explained by the fact that the increase in the amount of incident argon ions leads to a greater number of sputtered carbon atoms and thus to an increase in the growth rate. Then, with the increase of the nitrogen content in the plasma, we note a very slight increase of the deposition rate until a "critical" level. After this critical composition value, there is a minor decrease in the deposition rate, whatever the amount of argon initially introduced. This behavior is the consequence of the change of pulverization mode. It results from the modification of the target surface which causes the variation of the sputtering efficiency and thus of the deposition rate. This result is in agreement with previous studies [18, 19].

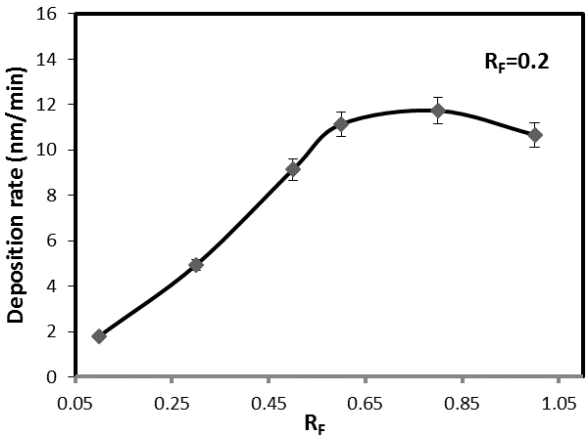

Fig. 2. Deposition rate of a-CN_x as a function of R_F

This work focuses specifically on the so-called "chemical" magnetron sputtering mechanism, particularly in the case of carbon-rich materials, because there is a variation between the binding energy of the reactive gas and the sputtered atoms [3]. If a target is bombarded with chemically reactive species, chemical effects must be taken into account. In this case, two opposite reactions can occur:

Chemical reactions between target atoms and reactive gas can form "CN^+, $C_2N_2^+$…" species that are weakly bounded to the surface and easily sputtered. This results in an increase in the sputtering efficiency. Otherwise, the newly formed compounds may have strong bonds with the target atoms and, therefore, a higher surface binding energy, resulting in a decrease of sputtering rate [8]. In general, the sputtering intensity of the elements decreases considerably when compounds form on the target due to the lower sputtering yield of the relative compounds. This was nevertheless not the case in the reactive sputtering of carbon nitride films. As nitrogen gas was incorporated into the sputtering atmosphere,

reactive nitrogen ions, atoms and molecules were formed and reacted on the target, in the discharge and on the substrate surface with carbon atoms. It can be suggested that the higher partial nitrogen pressure caused a higher nitrogen flux to the substrate, leading to the formation of carbon nitride films [20]. On the other hand, we suggest that target atoms are removed from the surface by collisions between projectiles and/or recoil of produced atoms and the atoms in the near-surface layers of the target material, resulting in a decrease in sputtering efficiency.

Figure 3a, shows a typical experimental RBS spectrum and the corresponding simulation for R_F= 1. As can be seen from Figure 3b, RBS results give the composition variation of thin films deposited in different gas mixtures. By increasing R_F from 0.1 to 0.6, the N content in the films increases from 0 to 42 at. %. After this, and when R_F increases beyond the value of 0.6, the N content decreases. Many approaches include interactions between nitrogen ions and carbon surfaces. Nitrogen is known to create chemical bonds with carbon atoms during ion bombardment, to generate volatile compounds. It was proposed that chemical sputtering was responsible for the observed nitrogen content limitations and the growth rate of carbon nitride films. Subsequently, CN and C_2N_2 molecules with optical emission spectroscopy and mass spectrometry were detected by a number of research groups, confirming the importance of chemical sputtering for the growth of carbon nitride films [21,22].We also find that traces of oxygen (O< 3 at. %) are present in the films deposited under argon-nitrogen plasma. We attribute this result to the presence of residual gases (oxygen, water vapor) in the deposition chamber and to the high reactivity of oxygen.

The nitrogen to carbon atomic ratio in a-CN_x films was determined as shown in Fig. 3c the incorporated nitrogen atoms in a-CN_x films were chemically bonded to carbon. N/C ratio was increased from 0.53 to 0.76 when R_F increases from 0.2 to 0.6, this was due to the impact of the increased amount of graphite receiving nitrogen.

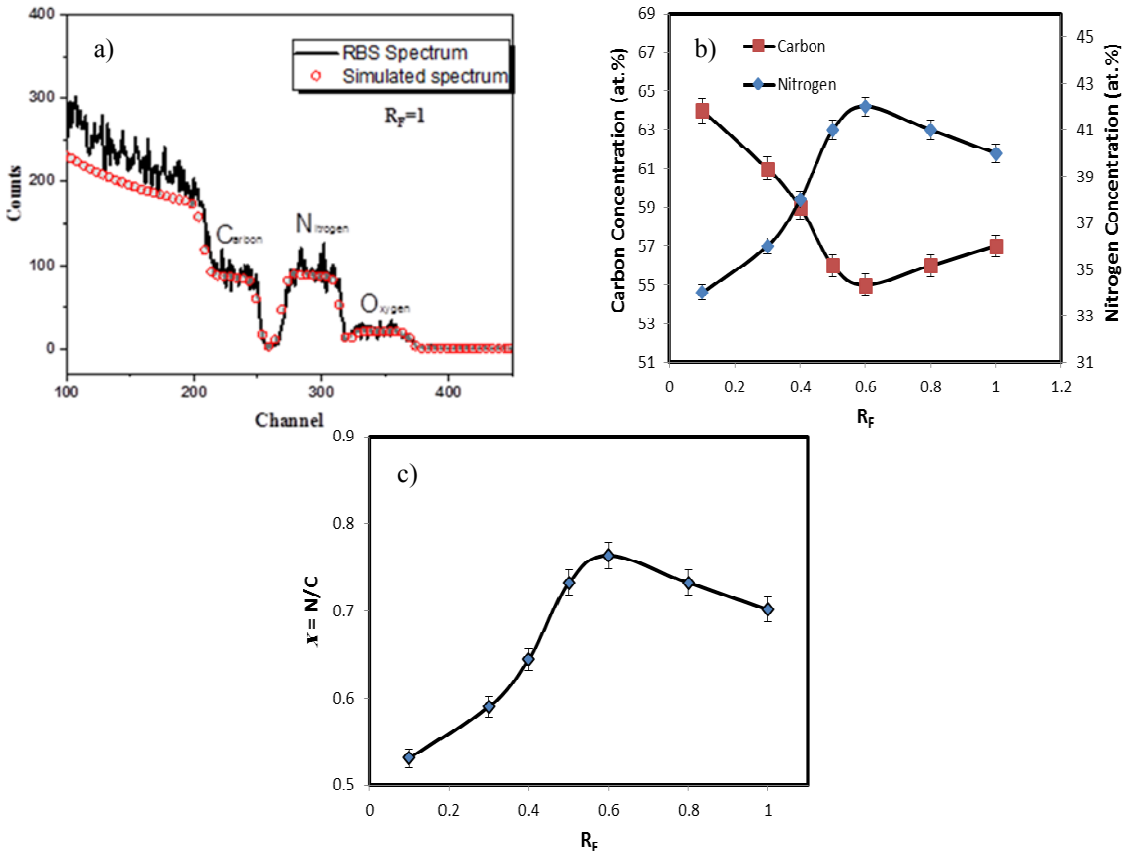

Fig. 3. a) Experimental and simulated RBS spectrum for R_F= 1 b) Composition of a-CNx films as a function of RF c) Ratio of the number of nitrogen and carbon atoms in a-CN_x films.

Then, the nitrogen carbon ratio decreased from 0.76 to 0.70 with the increase of R_F from 0.6 to 1. It is noted that in a previous study, the ratio was 0.75 but with deposition on substrates heated at 100°C [23]. A previous study found that calculated N/C ratios ranged between 1 and 1.3, but because silicon substrates were employed, it was unable to confirm whether this element was incorporated in the film [24].

ESR measurements afford information about the existence of unpaired electrons, as well as quantities, type, nature, surrounding environment, and behavior.

A typical ESR spectrum is shown in Figure 4 for R_F= 0.4. We saw clearly that the line shape is close to Lorentzian as it is generally the case of amorphous materials.

The spin density D_S and the peak-to-peak line width ΔH_{PP}, derived from ESR analysis for different R_F values are presented in Table I. The obtained spin density is in the order of 10^{17} cm^{-3}, however, the spin density observed in previous studies is estimated in the order of 10^{16} cm^{-3} [25, 26].When R_F increases, the spin density tends to be similar suggesting that the structures are more alike, this is due to an ordering of the sp^2 structures and less dangling bonds [27]. One can notice that spin density in some diamond like carbon (DLC) films is about 10^{20} cm^{-3} [28].

The average g-value, which reflects the orbit level occupied by the electron, is ~2.001 for the different deposited films. As reported by Suter et al. [29], the g value varied between 2.0034 and 2.0035.

Surface topography can be explored using Atomic Force Microscopy (AFM) with near-atomic resolution. It can measure the surface roughness of samples down to the Angström level. As shown in figure 5, 2D and 3D AFM image reveal the morphology of the materials in a total surface area of 5µm × 5µm. It is apparent that both surface roughness and surface morphology modifications are depending on the R_F variation.

Like films (sp^3), graphitic films (sp^2), and polymeric films (sp^1) can be described.

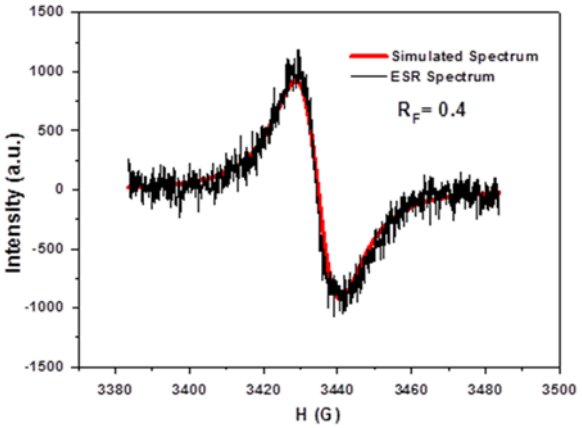

Fig. 4. ESR spectra of a-CN_x thin films for R_F= 0.4 owing

Figure 6a presents the infrared spectra of the different deposits in the range 500-3500 cm^{-1}. Three bands can be identified: the first one at 620 cm^{-1} typical of the Si (100) substrate surface, the second one at 730 cm^{-1} corresponding to Si-C vibration mode. The second order vibration mode of silicon is observed at 1120 cm^{-1}. The elongation vibrations of the CC and CN bonds are observed in this range [32]. FTIR absorption spectra are shown in Figure 6.a for R_F= 1.

Table 1. The spin density D_S and the peak-to-peak line width ΔH_{PP}:

R_F	g (G)		ΔHpp (G)	$D_S(10^{17}cm^{-3})$
0.2	2.000		15	5.16
0.4	2.002		15	5.23
0.6	2.001		15	5.21
0.8	2.000		12	4.20
1	2.002		9	5.61

Table 2. The variation of thickness, roughness and pore size of films for different R_F ratios.

R_F	Thickness (nm)	RMS (nm)	Pore size (nm)
0.1	27±10	0.917	2.996
0.3	74±10	-	-
0.5	137±10	1.030	6.184
0.6	167±10	-	-
0.8	176±10	13.82	32.448
1	160±10	-	-

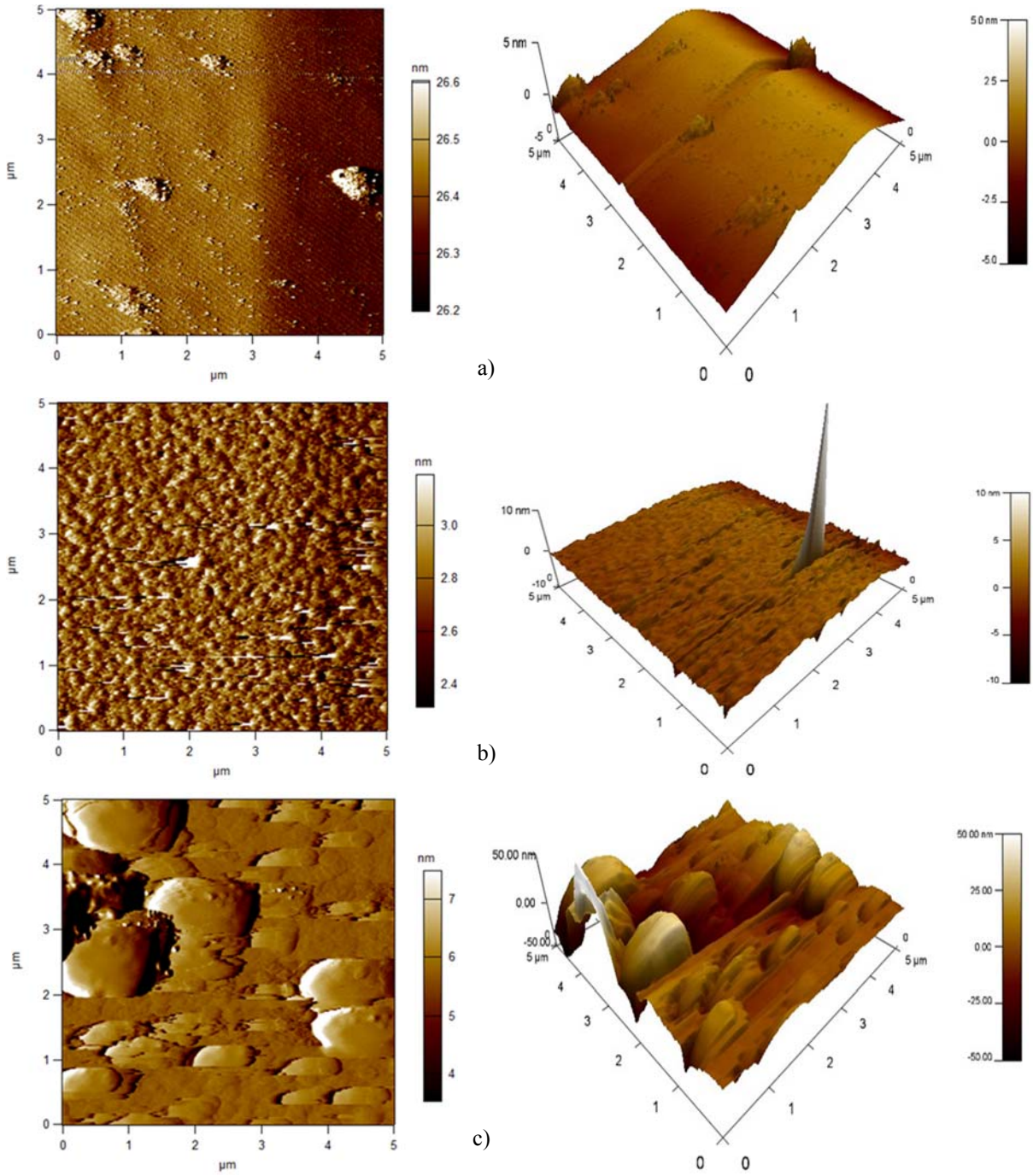

Fig. 5. 2D and 3D AFM topographic images of a-CN_x thin films for (a) R_F = 0.1, 0.3 , and 0.8

As can be seen from Figure 6b, the intensities of the peaks at 1323 cm^{-1} and 1403 cm^{-1} are attributed to the C-N and the C=N symmetric stretching bonds respectively. It can be said that the C-N and C=N bonds behave in opposite behaviors and always pass through an extremum. The obtained results agree with those of Teter et al. [33], the C=N frequency is found below 1500 cm^{-1}.

A narrowing of the D-peak at 1456.2 cm^{-1} is observed with the increase of R_F. This is attributed to the decrease of graphitic disorder and an ordering of the sp^2 structure [34]. One can also notice an increase of the intensity of the G-peak at 1595.9 cm^{-1} with the increase of R_F which is attributed to the graphitic vibrations of C=C.

There is a great interest in estimating structural disorder due to sp^2(C) sites. The evolution of the

I_D/I_G intensities ratio of the peaks attributed respectively to D and G bands is shown in Figure 6c. It was known that the (I_D/I_G) parameter is sensitive to the degree of structural order; the more ordered, the structure of the material, the more this parameter decreases, and vice versa. According to the literature, disorder increases with decreasing size of sp^2 sites.

These sites are formed because of the bond breakdown that occurs during ion bombardment when deposition takes place. Nitrogen atoms present in the plasma create substitutional bonds when bond cleavage occurs at the surface of the layers, which reduces the sp^2 sites and their size [35].

The decrease in the (I_D/I_G) ratio was observed for R_F values from 0.3 to 0.92, then it stabilises around 1, for R_F >0.3. In [36] it was shown that the decrease in the (I_D/I_G) ratio leads to a presence of sp^2 sites.

There is also a low-intensity absorption region at about 2300 cm^{-1}, which can be associated to the presence of cyano group (C≡N) such as -C≡N, -N≡C and -C=N- bonds [37]. The presence of this absorption region allows us to confirm that the nitrogen is bounded to the carbon in the deposited layers, making the structure harder [38, 39]. According to Riedel et al. and Patai [40, 41], at high nitrogen concentration, a peak at about 2200 cm^{-1} is frequently observed and is thought to be associated to CN.

The CN denotes the amount of sp^1 carbon in the films. This type of bonding generates bond-terminating sites, leading to a lack of connectiveness and a less densely packed structure in the films.

There is a low intensity absorption region at 3300 cm^{-1}, that can be associated with the OH or NH bond, suggesting low contamination inside the chamber or by the ambient air as soon as the deposits are extracted from the chamber [42]. Several studies have found D and G peaks in FTIR spectra. However, they demonstrated that the position of the D and G peaks can vary depending on the experimental conditions [43-45].

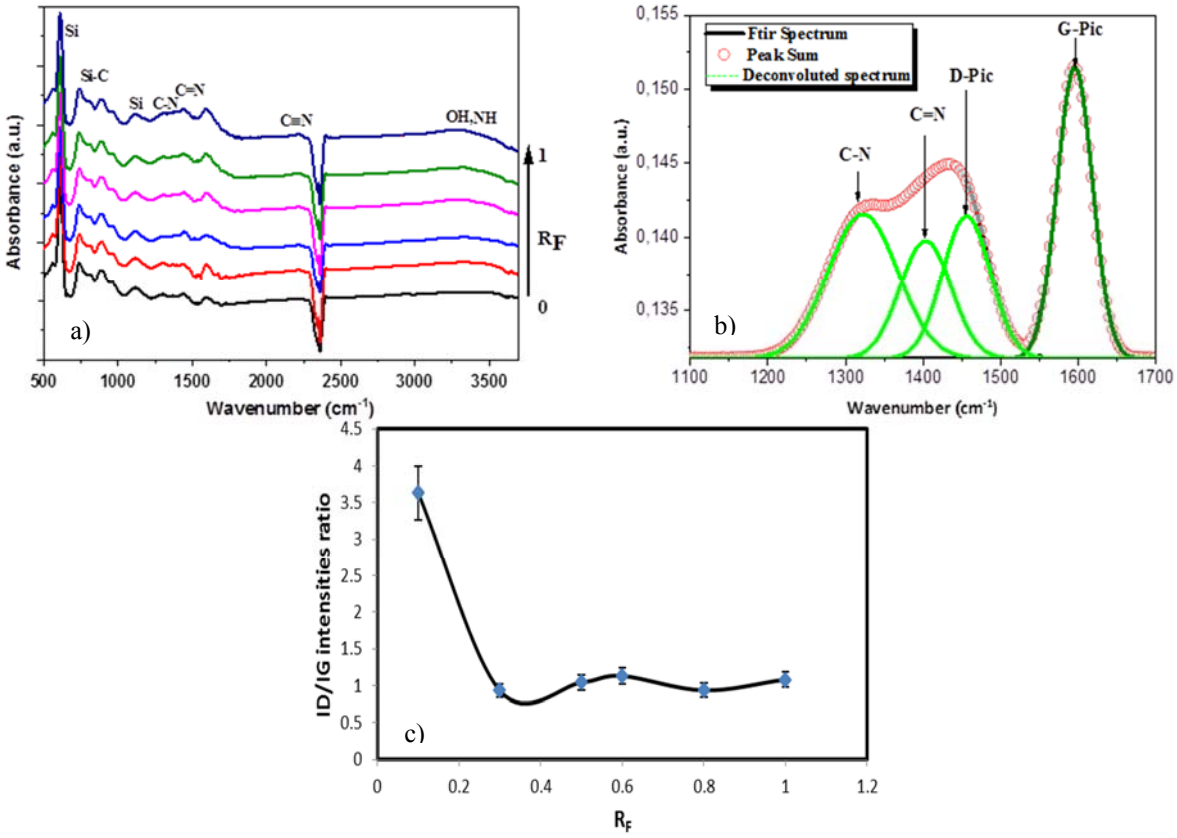

Fig. 6. a) FTIR absorption spectra of a-CN_x thin films for different R_F values b) Deconvolution of FTIR absorption spectrum of a-CN_x thin films in 1200-1700 cm^{-1} zone for R_F= 1 c) (I_D/I_G) intensities ratio of the Infrared D and G bands of the a-CN_x thin films as a function of different values of R_F.

3.2. Optical Measurement

The dependence between the photon energy and the optical absorption coefficient (α) for deposited films is expressed according to Tauc's law [46], by the relation 1:

$$(\alpha h\upsilon)^{1/n} = \beta(h\upsilon - E_g) \quad (1)$$

β is a constant, Eg is the optical gap [eV], and $h\upsilon$ is the photon energy, n is a factor that depends on the transition mode [47, 48]. According to Tauc's law, the variation in the absorption coefficient can be divided into three distinct regions:

1) A region of low absorption ($\alpha < 1$ cm^{-1}) in which absorption is due to defects and impurities present in the film.
2) A region in which the variation in absorption is due to states in the band tail, for 1 cm^{-1} < α < 104 cm^{-1}.
3) A region of high absorption (α >104 cm^{-1}). This region corresponds to the optical transitions between the valence band and the conduction band. These transitions are responsible for the absorption front at above λ= 303 nm [49].

In the visible range, the spectra show good transparency for $R_F < 0.5$. On the other hand, for $R_F > 0.5$, the deposited layers show the lowest transmittance (Figure 7a).

Comparing these results with the AFM analysis, one can say, the higher the surface roughness, the lower the transmittance. We, therefore, observe that the transmission of the films decreases in the visible range if R_F increases.

For amorphous materials, the indirect transition is acceptable according to Tauc's law. Therefore, we take $n = 2$ for our layers and we will have the relation 2:

$$(\alpha h\upsilon)^{1/2} = \beta(h\upsilon - E_g) \quad (2)$$

By extrapolating the linear part of $(\alpha h\upsilon)^{1/2}$ versus $h\upsilon$ plot to the x-axis, the value of Eg can be obtained, as shown in Figure 7b.

The parameter that characterizes the material disorder is Urbach's tail energy.

According to Urbach's law, the expression of the absorption coefficient is given by the relation 3:

$$\alpha = \beta \exp(h\nu/E_u) \quad (3)$$

By plotting ln (α) against (hν) in Figure 7c, one can determine the value of E_u by the relation 4:

$$\ln \alpha = \ln \alpha_0 + h\nu/E_u \quad (4)$$

When the disorder becomes too pronounced (e.g., with the appearance of dangling bonds or impurities in the material), the tails can become entangled. We will then define the notion of Urbach parameter (E_u) which corresponds to transitions between the extended states of the valence band and the localized states of the conduction band. E_u being the width of the band tail which characterizes the disorder. Urbach energy E_u can also be interpreted as the band width of the states located in the band gap [50, 51].

The evolution of the optical gap Eg as a function of R_F is reported in Figure 7d. The values of Eg are in the range of 3.59 to 3.63 eV. These values show that our films have a wide gap and are transparent in the visible range. This result is promising with the aim of developing anti-reflection layers or transparent protective layers.

The variation in the optical gap Eg is negligible (3.63-3.59= 0.04 eV) suggesting that the films are polymer-like carbon type (PLC), optimal for hemo-compatibility applications, with large optical gaps (>2.6 eV) and low spin densities (10^{16}-10^{17} cm^{-3}) [52]. It is clear that pore size has no effect on band gaps, as all films, regardless of pore size, have a band gap of about 3.6 eV. Different optical gap values (2-3.8 eV) [53, 54] and (3.2-4.3 eV) [55] have been registered by other authors.

These results suggested that the incorporation of nitrogen into the amorphous carbon enhances the optical band gap and this enhancement relies on the nature of C: N bond in the film. Moreover, it is consistent with previous works on CNx films, in which the band gap was found to be significantly dependent on the I_D/I_G ratio as well as sp^2 sites, as mentioned above [56, 57].

Let's remember that sp^3 rich diamond has an optical gap equal to 5.5 eV and sp^2 rich graphite has a zero optical gap, which allows us to predict that the deposited a-CN_x films have a high hardness due to the presence of sp^3 sites at the expense of sp^2 sites [58, 59].

Fig. 7d also shows that as the nitrogen rate increases, less disorder in a-CN_x thin films is observed. The decrease in sp^2 sites and consequently the disorder has been studied and confirmed by infrared measurements as shown earlier in this study.

3.3. Electrical Measurement

The electrical properties were investigated by two-point probe method.

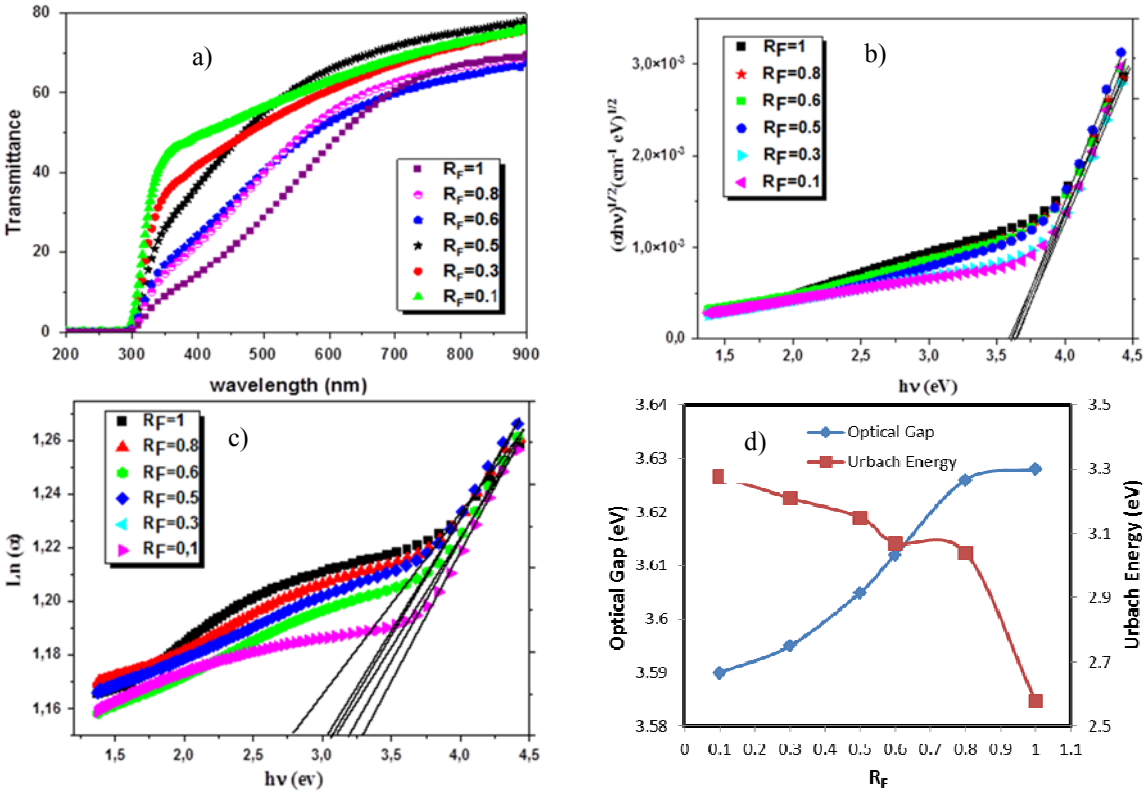

Fig. 7. a) Optical transmittance as a function of wavelength of a-CN_x thin films for different values of R_F b) Variation of $(\alpha h\upsilon)^{1/2}$ with the photon energy ($h\upsilon$) c) Variation of (Ln α) with the photon energy ($h\upsilon$) d) Variation of optical gap E_g and Urbach energy E_u as a function of different values of R_F

The evolution of the resistivity of a-CN_x thin films as a function of the ratio of the reactive gas flow rates R_F is shown in Figure 8a. There is an increase in resistivity from 15 to 87.4×10^{-3} Ω. cm of a-CN_x thin films for $0.1 < R_F < 0.8$ and a less decrease for $R_F > 0.8$. This is because increasing the pore size reduces electrical interaction between particles. Note that the resistivity values are lower than those obtained in other studies, as shown in Table 3. The low resistivity of a-CN_x films supports the development of electrical and opto-electronic devices.

The film resistivity was measured under different temperatures ranging between 60 and 100°C. The obtained results show that the resistivity of a-CN_x films is very sensitive to temperature. It decreases from 9×10^7 to 4×10^6 Ω. cm when the temperature increases from 60 to 100°C then the resistivity still constant Figure 8b. The incorporation of nitrogen enhances carbon nitride films conductivity [60]. This gives the opportunity to their use in electrical devices.

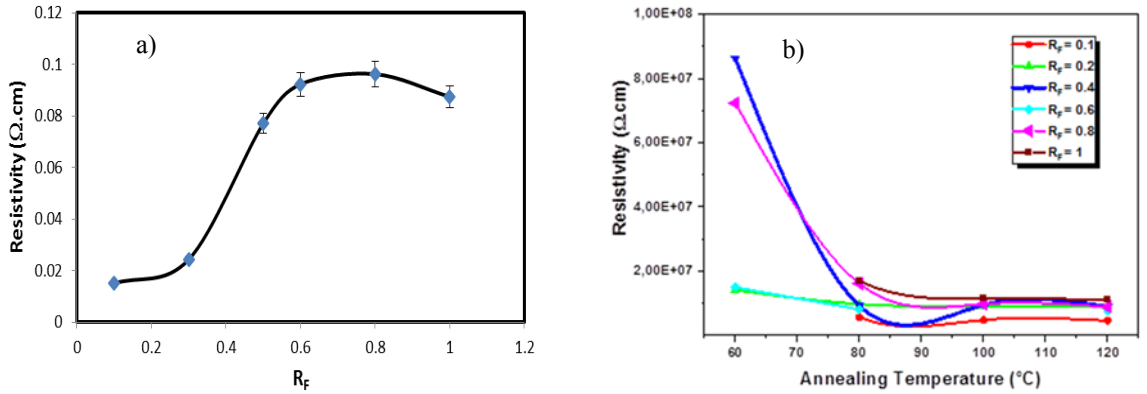

Fig. 8. a) Resistivity of a-CN_x thin films as a function of different values of R_F b) Resistivity versus annealing temperature of a-CN_x thin films deposited under different values of R_F

Table 3. The obtained resistivity values compared to literature ones.

	Resistivity (Ω . cm) at room temperature	**Resistivity (Ω . cm) from 60 to 120°C**
This study	15×10^{-4}-87.4×10^{-3}	4×10^{6}- 9×10^{7}
[35]	0.23-5.26	
[61]	$1x10^{7}$-$1x10^{12}$	

4. CONCLUSIONS

The objective of this work was to prepare and characterize amorphous carbon nitride (a-CN_x) thin films. Films were deposited by reactive radio frequency sputtering of a graphite target under the atmosphere of argon and nitrogen at different concentrations at room temperature. The highest nitrogen content in films was estimated to 42 at. % which is very rare.

High-quality films with spin density in the order of 10^{17} cm^{-3} were achieved at ambient temperature, a very promising result that was reproducible and compatible with device quality. The spin density was similar, suggesting that the structures were alike.

The surface state study by AFM showed an increasingly rough surface with increasing nitrogen concentration. For R_F= 0.1, the surface was flat and then became rougher for R_F >0.5.

Infrared spectroscopy measurement revealed that nitrogen atoms are embedded in the carbon bonding network with the presence of C-N, C=N and C≡N chemical bonds, as well as the D and G peaks, characteristic of the graphitic disorder in the layers and the graphitic vibrations of the C=C bonds. It was shown that the increase in the concentration of nitrogen, leads to a less disordered films.

The optical characterization showed good transparency in the visible range. The lowest value of the optical gap (3.59 eV) was obtained for R_F= 0.1, and the highest value (3.63 eV) for R_F= 1. These values show that deposited films have a wide band gap. The electrical conductivity was high compared to other studies. It was found that the increase in the pore size has minimal effect on band gaps. The increase in pore size, on the other hand, reduced the electrical resistivity.

REFERENCES

[1] Zhang, JT., Cao, C. B., Lv, Q., Li, C. and Zhu, H. S., "Optical and Electrical Properties of Carbon Nitride Films Deposited by Cathode Electrodeposition". J. Mater. Sci., 2003, 38, 2559-2562.

[2] Hernández-Torres, J., Gutierrez-Franco, A., P. González, G., García-González, L., Hernandez-Quiroz, T., Zamora-Peredo, L., Méndez-García, V. H., Cisneros-de la Rosa, A., "Photoluminescence and Raman Spectroscopy Studies of Carbon Nitride Films". J. Spectroscopy, 2017, 2016, 8.

[3] Contreras, E., Bolívar, F., Gómez, M. A., "Influence of Nitrogen Variation on the Microstructural, Mechanical and Tribological Properties of CNx Coatings Deposited by Dc Unbalanced Magnetron Sputtering". Surf. and Coat. Technol., 2017, 332, 414-421.

[4] C. J. Torng, J. M. Sivertsen, J. H. Judy, C. Chang, "Structure and Bonding Studies of the C:N Thin Films Produced by RF Sputtering Method".J. Mater. Res., 1990, 5, 2490-2496.

[5] Addie, A. J., Ismail, R. A., and Mohammed, M. A., "Amorphous carbon nitride dual-function anti-reflection coating for crystalline silicon solar cells." Scientific Reports, 2022, 12, 1-12.

[6] Kelly, P. J., and Arnell, R. D., Vacuum, 2000, 56, 159.

[7] Mróz, W., Burdyńska, S., Prokopiuk, A., Jedyński, M., Budner, B. and Korwin-Pawlowsk, M. L., "Characteristics of Carbon Films Deposited by Magnetron Sputtering". Acta Phys. Pol. A, 2009, 116, S-120.

[8] Anğay, F., Camelio, S., Eyidi, D., Krause, B., and Abadias G., "Structure, Electrical, and Optical Properties of Reactively Sputter-Deposited Ta-Al-N Thin Films". J. Appl. Phys., 2022, 131, 105303.

[9] Simon, A. H. "Sputter Processing". Handbook of Thin Film Deposition (Fourth Edition), ed. K. Seshan and D. Schepi, 2018, 195-230.

[10] Matsuoka, M., Isotani, S., Mansano, R. D., Sucasaire, W., Pinto, R. A. C., Mittani, J. C. R., Ogata, K. and Kuratani, N., " X-Ray Photoelectron Spectroscopy and Raman

Spectroscopy Studies on Thin Carbon Nitride Films Deposited by Reactive RF Magnetron Sputtering". WJNSE, 2012, 02, 92.

[11] Matsumoto, O., Kotaki, T., Shikano, H., Takemura, K., and Tanaka, S., J., "Synthesis of Carbon Nitride in Plasma Arc". Electrochem. Sot., 1994, 141, L16.

[12] Murahari, P., Fernandes, B. J., Kumar, K. D. A., Simon, R.F. and Ramesh, K., "Carbon Nitride for Photovoltaic Applications". AIP Conference Proceedings, 2020, 2265, 030645.

[13] He, XM., Shu, L., Li, WZ. et al. "Structure and Properties of Carbon Nitride Films Synthesized by Low Energy Ion Bombardment". J. Mater. Res., 1997, 12, 1595-1602.

[14] "SIMNRA User's Guide", Mayer, https://mam.home.ipp.mpg.de/.

[15] Teng, E., Jiaa, C., Eltoukhy, A., "Diamond-Like Carbon Overcoat for Magnetic Thin Film Recording Disks". Surf. and Coat. Tech., 1994, 68, 632.

[16] Mott, N. F., "Conduction in Non-Crystalline Materials". The Philosophical Magazine: A Journal of Theoretical Experimental and Applied Physics, 1969, 19-160, 835-852.

[17] Muhl S., Manuel Mendez J., "A review of the preparation of carbon nitride films". Diam. Relat. Mater., 1999, 8 ,1809-1830.

[18] Fenkera, M., Julinb, J., Petrikowski, K., and Richter, A., "Physical and Electrical Properties of Nitrogen-Doped Hydrogenated Amorphous Carbon Films". Vacuum, 2019, 162, 8.

[19] Rusop, M., Soga, T., and Jimbo, T., "The properties of Amorphous Carbon Nitride Thin Films Synthesized by Pulsed Laser Deposition with Various Preparation Conditions". Surf. Rev. and Let., 2005, 12, 333.

[20] Kusano, Y., Evetts, J. E., Somekh, R. E., Hutchings, I. M., "Properties of Carbon Nitride Films Deposited by Magnetron Sputtering". Thin Solid Films, 1998, 332, 56.

[21] St-Onge, L., Sing, R., Béchard,S., and Sabsabi, M., "Carbon Emissions Following 1.064 µm Laser Ablation of Graphite and Organic Samples in Ambient Air". Appl. Phys.A, 1999, 69, S913.

[22] Boueri, M., Baudelet, M., Yu, J., Mao, X., Mao, S., and Russo, R., "Early-Stage Expansion and Time-Resolved Spectral Emission of Laser-Induced Plasma from Polymer". Applied Surface Science, 2009, 255(24), 9566-9571.

[23] L., Wan and R. F., Egerton, "Preparation and Characterization of Carbon Nitride Thin Films". Thin Solid Films, 1996, 279, 34.

[24] Muhl, S., Gaona-Couto, A., Mendez, J. M., Rodil, S., Gonzalez, G., Merkulov, A., and Asomoza, R., "Production and Characterisation of Carbon Nitride Thin Films Produced by a Graphite Hollow cathode system." Thin Solid Films, 1997, 308, 228-232.

[25] Meng, L. J., and Santos, M. D., "Characterization of Titanium Nitride Films Prepared by D. C. Reactive Magnetron Sputtering at Different Nitrogen Pressures". Surf. Coat. Technol., 1997, 90, 64.

[26] Hahn, B. H., Jun, J. H., and Joo, J. H., "Plasma Conditions for the Deposition of TiN by Biased Activated Reactive Evaporation and Dependence of the Resistivity on Preferred Orientation". Thin Solid Films, 1987, 153, 115-122.

[27] Okajima, Y., "Estimation of Sputtering Rate by Bombardment with Argon Gas Ions". J. Appl. Phys., 1980, 51, 715.

[28] Sadki, A., Bounoh, Y., Theye, M. L., VonBardleben, J., Cernogora, J., and Fave, J. L., "Studies by Electron Paramagnetic Resonance Experiments of Defects in Hydrogenated Amorphous Carbon Films as a Function of Annealing"., 1996, 5, 439.

[29] Suter, T., Brázdová, V., McColl, K., Miller, T. S., Nagashima, H., Salvadori, E., and McMillan, P. F., "Synthesis, Structure and Electronic Properties of Graphitic Carbon Nitride Films." J. Phys. Chem. C, 2018, 122, 25183-25194.

[30] Fang, L., Jiang, Y., Zhu, S., Ding, J., Zhang, D., Yin, A., and Chen, P., "Substrate Temperature Dependent Properties of Sputtered AlN: Er Thin Film for In-Situ Luminescence Sensing of Al/AlN Multilayer Coating Health." Materials, 2018, 11, 2196.

[31] Shah, H. N., Jayaganthan, R., and Kaur,

D.," Influence of Reactive Gas and Temperature on Structural Properties of Magnetron Sputtered CrSiN Coatings"., Applied Surface Science, 2011, 257, 5535-5543.

[32] Schmidt, S., Czigany, Z.t, Wissing, J., Greczynski, G., Janzén, E., Jensen, J. I., Gueorguiev, I. and Hultman, L., "A comparative Study of Direct Current Magnetron Sputtering and High Power Impulse Magnetron Sputtering Processes for CNX Thin Film Growth with Different Inert Gases"., 2016, 64, 13.

[33] Teter, D. M., "Computational Alchemy: The search for New Super HardMaterials." MRS Bulletin, 1998, 23, 22-27.

[34] Barklie, R.C., Collins, M. and Silva, S.R.P., "EPR Linewidth Variation, Spin Relaxation Times, and Exchange in Amorphous Hydrogenated Carbon". Phys. Rev. B, 2000, 61, 3546.

[35] Aono, M., Takeno, T., and Takagi, T., "Structural, Electrical, and Optical Properties of Amorphous Carbon Nitride filmsPrepared Using a Hybrid Deposition Technique". Diam.Relat. Mater., 2006, 63, 120-124.

[36] Ferrari, A. C., Rodil, S. E., and Robertson, J. "Interpretation of Infrared and Raman Spectra of Amorphous Carbon Nitrides ". Phys. Rev., 2003, B67, 155306.

[37] Alnama, K., Alkhawwam A., and Jazmati, AK., "Investigation of Local Thermodynamic Equilibrium of Laser Induced Al_2O_3–TiC Plasma in Argon by Spatially Resolved Optical Emission Spectroscopy ". Acta Phys. Pol. A., 2011, 120, 545.

[38] Crunteanu, A., Charbonnier, M., Romand, M., Vasiliu, F., Panelica, D., Negoita, F., and Alexandrescu, R. "Synthesis and Characterization of Carbon Nitride Thin Films Obtained by Laser-Induced Chemical Vapor Deposition". Surf. Coat. Technol., 2000, 125, 301.

[39] Wang, C., Yang, S., and Zhang, J., "The Infrared Characteristics Investigation of Carbon Nitride Films.", 2008, 17, 174-179.

[40] Riedel, R., Kroke, E., Greiner, A., Gabriel, A. O., Ruwisch, L., Nicolich, J., and Kroll, P., "Inorganic Solid-State Chemistry WithMain Group Element Carbodiimides." Chem.Mater., 1998, 10, 2964-2979.

[41] Patai S., Rappoport Z., The Chemistry of Alkanes and Cyclocanes, John Wiley and Son, 1992.1079.

[42] Peponas, S., Benlahsen, M., and Guedda, M., "On the Delamination Dynamic of Sputtered Amorphous Carbon Nitride Films". J. Appl. Phys., 2009,106, 013525.

[43] Kaltofen, R., Sebald, T., and Weise, G., "Low-Energy Ion Bombardment Effects in Reactive RF Magnetron Sputtering of Carbon Nitride Films." Thin Solid Films, 1997, 308, 118-125.

[44] Taki, Y., Kitagawa, T., and Takai, O., "Shielded Arc Ion Plating and Structural Characterization of Amorphous Carbon Nitride Thin Films." Thin Solid Films, 1997, 304, 183-190.

[45] Schwan, J., Batori, V., Ulrich, S., Ehrhardt, H., and Silva, S. R. P., "Nitrogen Doping of Amorphous Carbon Thin Films." J. Appl. Phys., 1998, 84, 2071-2081.

[46] Tauc, J., Grigorovici, R., and Vancu, A., "Optical Properties and Electronic Structure of Amorphous Germanium". Phys. Status Solidi (b), 1966, 15, 627-637.

[47] Bhattacharyya, D., Chaudhuri, S., and Pal, A., "Bandgap and Optical Transitions in Thin Films from Reflectance Measurements", Vacuum, 1992, 43, 313-316.

[48] Sharma, A., Mehta, N. and Kumar, A., "Dielectric Relaxation in Se80-X Te20Sn-X Chalcogenide Glasses". J. Mater. Sci., 2011, 46, 4509-4516.

[49] Shahane, G. S., More, B. M., Rotti, C. B., and Deshmukh, L. P., "Studies on Chemically Deposited CdS1-XSEXMixed Thin Films". Mater. Chem Phys., 1997, 47, 263-267.

[50] Krishna, K. M., Ebisu, H., Hagimoto, K., Hayashi, Y., Soga, T., Jimbo, T., and Umeno, M. (2001). "Low Density of Defect States in Hydrogenated Amorphous Carbon Thin Films Grown by Plasma-Enhanced Chemical Vapor Deposition". Appl. Phys. Lett., 2001, 78, 294-296.

[51] Kundoo, S., Chattopadhyay, K. K., Banerjee, A. N., and Nandy, S. K., "Synthesis and Optical Characterization of Amorphous Carbon Nitride Thin Films by Hot Filament Assisted RF Plasma CVD". Vacuum, 2003, 69, 495-500.

[52] Ogata, K., Chubaci, J. F. D., and Fujimoto, F., "Properties of Carbon Nitride Films with Composition Ratio C/N= 0.5-3.0 Prepared by the Ion and Vapor Deposition Method" .J. Appl. Phys., 1994, 76, 3791-3796.

[53] Lin, D. Y., Li, C. F., Huang, Y. S., Jong, Y. C., Chen, Y. F., Chen, L. C., Bhusari, D. M., "Temperature Dependence of The Direct Band Gap of Si-Containing Carbon Nitride Crystalline Films". Phys. Rev. B., 1997, 56, 6498-6501.

[54] Muiva, C. M., Sathiaraj, T. S., and Mwabora, J. M., "Chemical Bond Approach to Optical Properties of Some Flash Evaporated Se100-XSbX Chalcogenide Alloys". Eur. Phys. J. Appl. Phys., 2012, 59, 10301.

[55] Wicher, B., Chodun, R., Trzcinski, M., Nowakowska-Langier, K., Lachowski, A., andZdunek, K., "Applications Insight into the Plasmo Chemical State and Optical Properties of Amorphous CNxFilms Deposited by Gas Injection Magnetron Sputtering Method." Appl. Surf. Sci., 2021, 565, 150540.

[56] Majumdar, A., Bogdanowicz, R., Mukherjee, S., and Hippler, R., "Role of Nitrogen in Optical and Electrical Band Gaps of Hydrogenated/Hydrogen Free Carbon Nitride Film." Thin Solid Films, 2013, 527, 151-157.

[57] Hayashi, Y., Rahman, M. M., Kaneko, K., Soga, T., Umeno, M., and Jimbo, T., "Deposition of Amorphous CNx by DC and RF Plasma Sputtering Using a RF Radical Nitrogen Beam Source." Diam. Relat. Mater., 2002, 11, 1178-1182.

[58] M. S. Dresslhaus, G. Dresslhaus and P. C. Eklund, Science of Fullerenes and Carbon Nanotubes (Academic Press, 1996).

[59] Kelly, B. T. Physics of Graphite, Applied Sciences Publishers, 1981.

[60] Lanter, W. C., Ingram, D. C., and DeJoseph, C. A., "Amorphous Carbon Nitride for High-Temperature Capacitor Dielectric" Diam. Relat. Mater., 2006, 15, 259-263.

[61] Kikuchi, Y., Chang, X., Sakakibara, Y., Inoue, K. Y., Matsue, T., Nozawa, T., and Samukawa, S., "Amorphous Carbon Nitride Thin Films for Electrochemical Electrode: Effect of molecular structure and substrate materials" Carbon, 2015, 93, 207-216.